J Orthop Res. Author manuscript; available in PMC 2014 March 13.

Published in final edited form as:
J Orthop Res. 2011 February ; 29(2): 289–296. doi:10.1002/jor.21220.

Scleraxis Expression Is Coordinately Regulated in a Murine Model of Patellar Tendon Injury

Alexander Scott[1,2,3], **Arthur Sampaio**[1,2], **Thomas Abraham**[4], **Chris Duronio**[1], and **Tully M. Underhill**[1,2,3]

[1]Biomedical Research Centre, Vancouver, Canada

[2]Department of Cellular and Physiological Sciences, UBC, Vancouver, Canada

[3]Centre for Hip Health and Mobility, Vancouver Coastal Health Research Institute, Vancouver, Canada

[4]The James Hogg Research Centre, Heart & Lung Institute at St. Paul's Hospital, University of British Columbia, Vancouver, Canada

Abstract

This study investigated the expression of scleraxis in a murine model of patellar tendon injury in which the central third of the patellar tendon was unilaterally injured. The presence of tendon pathology was assessed using dual photon microscopy, conventional histology and micro CT. Tendon pathology was also quantified noninvasively over a 12-week period using high-frequency ultrasound and laser Doppler flowmetry. Gene expression (Scx, Tnmd, and Col1a1) was determined at defined end-points (1, 4, 8, and 12 weeks) using qPCR on RNA from individual patellar tendons on injured and uninjured sides. There was significant development of tendon pathology as gauged by ultrasound and laser Doppler over 12 weeks. Injured tendons demonstrated significant histological and microCT evidence of pathological change, and disorganized collagen with reduced density. The expression of Scx and Col1a1 was unchanged at 1 week, significantly upregulated at 4 and 8 weeks, and had returned to baseline by 12 weeks. Tnmd expression was unchanged at 1 week, and significantly increased at 4, 8, and 12 weeks. Patellar tendon injury was associated with marked increases in the expression of Scx, Tnmd, and Col1a1. Our data suggest new roles for Scleraxis in coordinating the response to injury in the pathogenesis of tendon disorders.

Keywords

scleraxis; patellar tendon; mouse model

INTRODUCTION

Tendon injuries occur frequently among athletes and workers and represent a spectrum of conditions seen frequently by rheumatologists including paratendonitis, chronic tendinosis,

✉Correspondence to: Alex Scott, PhD, Dept. of Physical Therapy, University of British Columbia, Vancouver, BC, Canada, ascott@mail.ubc.ca, phone: +1 604 875 4111 Ext. 21810, fax: +1 604 675 2576.

and tendon rupture[1]. Chronic tendon injuries can be significantly disabling, leading to lost time from work, physical inactivity, and early retirement from sports or labor [2–5].

The pathogenesis of many chronic tendon injuries remains poorly understood [6,7]. Biopsy material from surgical patients reveals a cluster of histological characteristics known as tendinosis, reflecting the essentially noninflammatory picture of chronic (> 3 months) injuries [4,5,8–10]. Commonly observed changes in chronic tendon injuries include adipose and fibrocartilaginous metaplasia, variable tenocyte density including both proliferation and apoptosis, disorganized collagen and reduced total collagen content, and proliferation of cells from paratendinous and neurovascular tissue [11–13]. This picture is consistent with a failed healing response model of tendon injury [14]. In this model, an injury—whether acute or due to insidious periods of overuse and matrix weakening and remodeling—triggers a repair and remodeling response which leads to imperfect estoration of tendon phenotype and long-term structural abnormality.

Studies of tendon biology and pathology have been hampered by lack of a consistent tendon phenotype marker. Traditionally, tendon is characterized morphologically by its abundant and well-organized collagen fibers, elongated and interconnected fibroblasts (tenocytes), and relative avascularity [15]. Recently, scleraxis (Scx) was identified as a master regulator of embryonic tendon [16–18]. Scx encodes for an E-box transcription factor required for early tendon development, being present in tendon progenitor cells of mouse limb bud from E11.5 onwards and continuously in tendon thereafter into adulthood [18]. Scx knock-out mice display dramatically reduced formation of load-bearing tendons, and reduced or absent expression of other tendon related genes including Col1a1 (type I collagen) and Tnmd (tenomodulin) [17]. Although Scx clearly plays key roles in tendon development, its role in adulthood—including the possibility of coordinate regulation during the response to injury —has not been extensively studied [19].

Therefore, we aimed to assess the extent of Scx expression in relation to tendon injury and repair in a novel murine model. We found that Scx was coordinately expressed following injury, over a prolonged time course in concert with an evolving tendon repair response. The findings support a novel role for SCX in injured tendon.

MATERIALS AND METHODS

Surgery

All animal procedures were carried out with the approval of the local animal ethics committee. The surgical procedure was based on a previously reported protocol.20 Forty female CD-1 mice were obtained at 8 weeks of age (Charles River, St. Constant, Canada) and used at 10 weeks of age. All mice underwent the surgical procedure, and the contralateral uninjured limb served as a control. Mice were then placed under isoflurane, and buprenorphine (0.1 mg/kg) and saline (0.5 ml) were injected subcutaneously. Using sterile surgical preparation, a 5mm incision was made over the shaved medial knee in order to avoid injuring the skin directly over the tendon. The tendon was exposed by laterally shifting the skin opening, and a number 11 blade passed through the lateral and medial retinacula and directly behind the patellar tendon. A 0.5mm biopsy punch (Shoney Scientific,

Waukesha, WI) was used to create a defect in the central part of the tendon, using the blade as a backing. The skin was apposed with a single sterile wound clip (9mm Autoclips, Becton-Dickinson, Franklin Lakes, NJ) placed medial to the knee. After 1 week, any remaining wound clips were removed. Animals were randomly assigned to time points at which they were euthanized.

Ultrasound Imaging

Ultrasound imaging was used to qualitatively and quantitatively monitor the response to injury. Under isoflurane, the mouse was placed on a custom plinth with a soft strap passing around the chest and under the forelimbs, with the lower limbs submerged in a 37°C water bath. Sagittal images of the right (injured) patellar tendon at baseline and at 1, 2, 3, 4, 10, and 12 weeks were obtained with a 35MHz water path probe. The sweep angle was 153 and image capture frequency was 80 MHz. The onboard digital caliper function was used to measure tendon anterior–posterior diameter (thickness) as an objective indicator of tendon pathology [21].

MicroCT Analysis

MicroCT analysis was used to confirm the location and extent of patellar tendon injury (Fig. 1). Mice were euthanized by CO2 inhalation and tendons dissected with bony attachments (patella and tibia) intact. The specimen was placed in 2.5% iodine for 3 h at 43C, then pinned flat on styrofoam and submersed in a 2 ml tube filled with sunflower oil. Tendons were scanned for their entire length at 45 kV, for 12.5 min (VivaCT, Scanco, Brüttisellen, Switzerland). In a subset of tendons, bony attachments were also included in the scan, and the tendon and bone thresholded to generate a binary image. For thresholding, sigma=8 and support=1 were used, with the lower threshold set at 158 and the upper threshold at 1,000. In optimization studies, the reduced X-ray lucency resulting from a 3-h incubation in iodine solution was found to occur preferentially in the water soluble components (e.g., tendon, fascia) but relatively excluded from fatty tissues (e.g., paratendinous tissue), thereby increasing the contrast between these tissue layers and allowing them to be separately assessed. The cross-sectional area for each tissue compartment (tendon and paratendon) was traced with the onboard software and calculated for the right (injured) and left (uninjured control) tendons of a subset (n=10 mice) 4 weeks after injury at the patellar tendon midpoint for both tendon and paratendon.

Blood Flow Monitoring

Blood flow was measured at 1mm depth using a laser Doppler flowmeter with tissue spectroscopy capability (O2C 1212, LEA Medizintechnik, Inc., Giessen, Germany) with LF-1 probe (1mm depth). The patellar tendon was clearly visible through the shaved, overlying skin, allowing the probe to be placed directly over the injured patellar tendon midportion. Scans were conducted under the same ambient lighting conditions, and following automatic correction for background illumination. Values for tendon blood flow were expressed in arbitrary units (AU) for the right (injured) and left (uninjured control) tendons.

Histology

Ten tendons (left and right, from five animals) were dissected at 16 weeks to examine for the presence of chronic histopathological changes [22]. All injured tendons were macroscopically abnormal on dissection. Tendons were fixed in paraformaldehyde, paraffin embedded, sectioned at 5 micron thickness, and stained with hematoxylin and eosin (H&E), Alcian blue (pH 2.5) for sulfated glycosaminoglycan with fast nuclear red counterstain, or picrosirius red for collagen. A modified Bonar scale [23] was used to quantitate the extent of tendon pathology as visualized using the three stains. The scale assigns a value of 0 (normal) to 3 (abnormal) for cellularity, collagen, vascularity, and glycosaminoglycan, and has been shown to be a valid and reliable indicator of chronic tendon pathology [22].

Collagen Analysis

Collagen structures in the histological specimens were visualized using second harmonic generation (SHG) microscopy [24]. A mode-locked femto-second Ti:Sapphire Tsunami (Spectra-Physics, Mountain View, CA) synchronously pumped by a Millenia Xs J (Spectra-Physics) diode-pumped solid-state laser capable of delivering up to 10W pumping power at 532nm was used. The Tsunami laser produced pulses of 100-fs width between 790 and 950 nm. The average power at different wavelengths was recorded by a Spectra-Physics 407a power meter. Wavelength identification and selection were performed with an IST laser spectrum analyzer (IST, Horseheads, NY) coupled to a TDS 210 oscilloscope (Tektronix, Beaverton, OR). The laser output was attenuated using neutral density filters (New Focus, San Jose, CA) and the average power maintained below the damage threshold of the samples. The power attenuated laser was directed to a Leica AOBS RS scan head (4,000 Hz) coupled with Leica upright microscope system (Heidelberg, Germany). The laser beam was focused on the specimen through a Leica 20×/0.7 Plan-Apochromat oil immersion objective. Upon entering the Leica microscope system, the laser beam was directed to the scanning mirrors, then through a 670nm long pass dichroic mirror (RSP 670, Leica) and subsequently focused through the objective lens. Leica Confocal Software TCS SP2 was used for image acquisition. SHG signal in the forward direction originating from the histological specimens was captured using a nondescanned detector in thetransmission geometry. In this nondescanned PMT detector (R6357, Hamamatsu, Shizuoka, Japan), a 440/20nmband pass filter (MP 440/20, Chroma Technology, Bellows Falls, VT) was used to collect the SHG signal. All SHG spectral data were generated using the descanned PMT detector (R6357, Hamamatsu) located inside the scan head where the emission signals were delivered through the AOBS detection system with the maximum confocal pinhole setting at 600 _m via the spectral dispersion prism. The gain and offset of the PMTs were adjusted for optimized detection using the color gradient to avoid pixel intensity saturation and background. Images (8 bit) were acquired at 10 s per 512×512 pixels.

The SHG signals from collagen structures have been shown to strongly depend on the collagen organization where collagen molecular density scales as a square-root of SHG signal intensity [25,26]. In order to determine the extent of collagen organization, we studied fixed samples from eight injured mice and eight control mice at 16 weeks post-injury. We recorded SHG images in four different areas for each sample, which resulted in 32 measurements in each case. We applied a noise removal filter with kernel size of 5×5 to

define the boundary between foreground and background, and the lower threshold in the histogram was set to 10% of the highest pixel intensity value. The total SHG signal intensity values thus generated were normalized by the cropped collagen area (square microns) and expressed in AU.

RNA Isolation and Quantitative PCR

At 0, 4, 8, and 12 weeks, right (injured) and left (uninjured control) tendons were dissected using a sterile blade and flash frozen in liquid nitrogen. Tendons were powdered in a tissue mill (Mikrodismembrator S, Sartorius, Germany) for 30s at 3,000 RPM in cryogenic tubes (Nalgene, Rochester, NY), then placed in 1ml Trizol. RNA was extracted according to the manufacturer's instructions and purified using RNEasy columns (Qiagen, Mississauga, Canada) and RNA was reverse transcribed using the High Capacity cDNA Reverse Transcription kit (Applied Biosystems, Foster City, CA), as previously reported.27 Gene expression was quantitated using qPCR on an ABI (Applied Biosystems) 7500 Fast system with custom ABI TaqMan MGB probe and primer sets for Scx and Col1a1 (Table 1), and proprietary ABI "On Demand" probe and primer sets for TNMD (00491594 m1) and 18s (cat#4308329). Expression was determined using the relative quantitation method and gene expression was normalized to 18s abundance as previously reported [27].

Statistical Analysis

To examine differences in gene expression, tendon thickness and tendon blood flow, a 1-way ANOVA was used followed by Bonferonni-corrected paired tests comparing matched right and left values for each variable. A paired t-test was used to detect differences in Bonar score, collagen density, and tendon/paratendon cross-sectional area. Statistical significance was predetermined at $p<0.05$.

RESULTS

At present, research into new treatments for tendon injuries is hampered by the lack of suitable small animal models, especially those in which genetically modified animals are available. To address this deficiency we have adopted a surgical model of patellar tendon injury in mice and characterized relevant molecular changes associated with this pathology.

Macroscopic Analyses

The injury procedure was well tolerated by animals, with no observable defect in cage mobility observed after cessation of anesthesia. Upon dissection, injured tendons appeared macroscopically abnormal compared to uninjured tendons at all time points, having a hyperemic region corresponding to the original defect site, as well as a more generalized thickened and/or yellowed appearance.

Ultrasound Appearance of Injured Tendon

Ultrasound demonstrated the acute onset and gradual resolution of tendon pathology over time, but with persistence of structural abnormality at the conclusion of the study (Fig. 2). Qualitative findings indicative of pathology which occurred in injured tendons included hypoechoic areas, collagen defects, and tendon bowing. Objectively, tendon thickness was

significantly increased by week 1 ($p<0.0001$) and gradually returned toward baseline over a 12-week period. Tendons remained on average twice as thick as controls at 12 weeks. These changes are consistent with chronic human tendon injuries, specifically in the fact that even 12 weeks post-surgery there were still marked changes in tendon structure.

Tendon Blood Flow

Blood flow was significantly increased in the injured patellar tendon compared to the uninjured side at 1 week ($p<0.001$), and gradually declined toward baseline over the ensuing weeks, but remained elevated even at 12 weeks ($p<0.05$) (Fig. 2). These observations are congruent with those of the ultrasound findings, in that the healing time is prolonged, and extended beyond the acute inflammatory phase.

MicroCT Appearance of Injured Tendon

MicroCT imaging of isolated tendons was used to evaluate pathological tendon changes (Fig. 3). Abnormalities including thickening, variability in lucency and irregularity of tissue borders, were present in both the tendon proper, and the anterior and posterior paratendinous tissues. Tendon cross-sectional area was increased to a similar degree as that observed using noninvasive ultrasound measures. However, the microCT analyses in comparison to ultrasound provided additional information on the extent and location of tendinous thickening (described in Fig. 3D).

Tendon Histology

The surgical model employed herein was designed to provide an acute injury stimulus, enabling efficient analysis of the evolution of cellular and molecular changes within injured patellar tendon. Histological analysis showed increased hypercellularity and collagen disruption in the injured tendon in comparison to control (Fig. 4A–D). Alcian blue staining also revealed the presence of chondrocytes within the paratendon (Fig. 4E). Furthermore, within the paratendon, sites of synovial and adipocyte proliferation were apparent (Fig. 4F). The Bonar score was 4.8+/−0.67 in injured tendons, and 0.6 +/− 0.43 in uninjured tendons. Together, these findings indicate that the murine patellar tendon injury model provides hallmarks remarkably similar to that observed in chronic human tendon injury.

Collagen Analysis

The SHG emission spectrum was used to evaluate collagen fibrillar organization and density. The wavelength scan of normal and injured tendons showed a highly specific SHG signal manifested by a narrow peak at 440nm (Fig. 5). This SHG signal was found to be spectrally clean arising only at the expected wavelength of 440nm which was exactly at the half the pumping wavelength of 880 nm. The SHG signal strength of normal tendons was found to be up to five times stronger than injured tendons, indicating that the collagen density was reduced in pathologic samples ($p=0.004$). Injury appeared to cause an excessive degradation and disarray of the collagen fibers particularly in the area of the tendon which was originally injured (central third). In contrast, areas of the injured tendon which were distant from the site of the original lesion (i.e., central third) demonstrated normal tendon morphology and a collagen density which was unchanged from controls (201 +/−21 vs. 191 +/−19 AU, n.s.).

Analysis of Scx, Tnmd, and Col1a1 Expression

Scx, Tnmd, and Col1a1 are all expressed during tendon development and in adult tendon; however, their expression has not been extensively assessed in relation to tendon injury. To assess gene expression, the patellar tendons were grossly dissected. The total RNA values were 37.65 (1.26) ng/l and average 260/280 ratio was 1.82 (0.06). Expression of 18s was unchanged at all time points. Analysis of Scx and Tnmd using qPCR showed a coordinated pattern of expression, with no change at 1 week, significant increases at 4 and 8 weeks ($p<0.05$), and returning to baseline at 12 weeks (Fig. 6). In contrast, Tnmd expression peaked later (8 weeks, $p<0.001$) and remained significantly upregulated at 12 weeks post-surgery ($p<0.01$). The injured tendon exhibited coordinated expression of Col1a1, Scx, and Tnmd, in association with multiple features of chronic tendon injury.

DISCUSSION

The creation of a partial defect in the mouse patellar tendon resulted in protracted increases in expression of Scx and associated genes, along with persistent ultrasound and microCT thickening of tendon and paratendon, increased blood flow, reduced collagen density, and histopathologic evidence of chronic tendon pathology. This study therefore demonstrates a potential role for Scx in a relevant murine model of tendon injury.

SCX, a transcriptional regulator, is abundantly expressed in embryonic and adult tendon [16]. The current article demonstrates that Scx is coordinately re-expressed after injury. The later time course of Scx expression suggests that it may be regulating transcription of tenocyte genes as cells differentiate within the repair tissue. The cell populations which contribute to tendon repair are not yet known, but roles have been postulated both for local tenocyte activation and proliferation, and recruitment of perivascular cells [28–30]. Presumably, once recruited or activated at the repair site these cells may undergo differentiation toward the tendon lineage. Indeed, tendons harbor pluripotent cells which may contribute not only to repair, but also to the pathological metaplasia observed following injury [31]. Further work is clearly required to identify the source and ultimate fate of Scx-expressing cells in injured tendon.

The injury stimulus to the central third of the patellar tendon resulted in persistent ultrasound and microCT abnormalities, increased blood flow, reduced collagen density, and histopathology consistent with chronic human tendon injuries. Here we reasoned that chronic tendon pathology may result from a failed healing response to an acute insult. Indeed, acutely injured human patellar tendon displays pathological changes up to 10 years following injury [32]. Our results support the use of a partial patellar tendon rupture as a valid injury model, at least for studying events up to 16 weeks after injury. Thus, the murine model will provide a useful tool with which to manipulate tendon biology to study emerging treatments to promote recovery from tendon injury.

We used harmonic generation imaging to visualize the fibrillar structure of collagen in histological specimens. Highly ordered fibril-forming collagens produce specific SHG signals without the need for any exogenous label [24,33]. The high specificity of SHG signals for fibrillar collagens results in an intrinsically low background in the images which

enables very sensitive measurements. In comparison, immunolabeling procedures for extracellular matrix components are less quantitative despite their specificities, since these methods are highly sensitive to the accessibility of the epitope in antigens recognized by the antibodies. In addition, bright field or fluorescent images of immunolabeled tissue samples are always convolved with a significant amount of background. Analysis of highly specific SHG signal in our studies demonstrated that the collagen density was significantly reduced in tendons even at 16 weeks after injury, confirming the presence of chronic tendon abnormality in this injury model. We anticipate much future use of SHG in the field of tendon research.

Expression of Scx and related genes showed coordinated regulation in relation to an extensively validated mouse patellar tendon injury model, representing a potentially important new function for Scx in post-natal tendon pathology and physiology.

Acknowledgments

The study was funded by a Canadian Institutes of Health Research (CIHR) Operating Grant Priority Announcement (Institute of Musculoskeletal Health and Arthritis). A Scott received fellowships and trainee awards from CIHR and the Michael Foundation for Health Research. TMU received an Investigator award from the Arthritis Society. TA received salary support from Providence Health Care and the James Hogg Research Centre, Heart and Lung Institute at St. Paul's Hospital.

References

1. Hazleman, B., Riley, G., Speed, CA. Soft tissue rheumatology. Oxford: Oxford University Press; 2004.
2. Tallon C, Coleman BD, Khan KM, et al. Outcome of surgery for chronic achilles tendinopathy. A critical review. Am J Sports Med. 2001; 29:315–320. [PubMed: 11394602]
3. Cook JL, Khan KM, Harcourt PR, et al. A cross sectional study of 100 athletes with jumper's knee managed conservatively and surgically. The Victorian Institute of Sport Tendon Study Group. Br J Sports Med. 1997; 31:332– 336. [PubMed: 9429013]
4. Maffulli N, Wong J, Almekinders LC. Types and epidemiology of tendinopathy. Clin Sports Med. 2003; 22:675–692. [PubMed: 14560540]
5. Jarvinen M, Jozsa L, Kannus P, et al. Histopathological findings in chronic tendon disorders. Scand JMed Sci Sports. 1997; 7:86–95. [PubMed: 9211609]
6. Banes, AJ., Tzsuzaki, M., Wall, ME., et al. The molecular biology of tendinopathy: Signaling and response pathways in tenocytes. In: Woo, SL.Renstrom, P., Arnoczky, SP., editors. Tendinopathy in athletes. Malden: Blackwell Publishing; 2007.
7. Lavagnino M, Arnoczky SP. In vitro alterations in cytoskeletal tensional homeostasis control gene expression in tendon cells. J Orthop Res. 2005; 23:1211–1218. [PubMed: 15908162]
8. Chard MD, Cawston TE, Riley GP, et al. Rotator cuff degeneration and lateral epicondylitis: A comparative histological study. Ann Rheum Dis. 1994; 53:30–34. [PubMed: 8311552]
9. Galliani I, Burattini S, Mariani AR, et al. Morphofunctional changes in human tendon tissue. Eur J Histochem. 2002; 46:3–12. [PubMed: 12044045]
10. Riley GP, Harrall RL, Constant CR, et al. Tendon degeneration and chronic shoulder pain: Changes in the collagen composition of the human rotator cuff tendons in rotator cuff tendinitis. Ann Rheum Dis. 1994; 53:359–366. [PubMed: 8037494]
11. Khan KM, Cook JL, Bonar F, et al. Histopathology of common tendinopathies. Update and implications for clinical management. Sports Med. 1999; 27:393–408. [PubMed: 10418074]
12. Scott A, Ashe MC. Common tendinopathies in the upper and lower extremities. Curr Sports Med Rep. 2006; 5:233–241. [PubMed: 16934204]

13. Scott, A., Khan, KM., Cook, J., et al. Human tendon overuse pathology: Histopathologic and biochemical findings. In: Woo, SL.Arnoczky, SP., Renstrom, P., editors. Tendinopathy in athletes. Malden, MA: Blackwell Publishing Ltd; 2007. p. 69-84.
14. Nirschl, RP. Patterns of failed healing in tendon injury. In: Leadbetter, W.Buckwalter, J., Gordon, S., editors. Sports induced inflammation: Clinical and basic science concepts. Park Ridge, IL: American Academy of Orthopaedic Surgeons; 1990. p. 577-585.
15. McNeilly CM, Banes AJ, Benjamin M, et al. Tendon cells in vivo form a three dimensional network of cell processes linked by gap junctions. J Anat. 1996; 189(Pt 3):593–600. [PubMed: 8982835]
16. Pryce BA, Brent AE, Murchison ND, et al. Generation of transgenic tendon reporters, scx gfp and scx ap, using regulatory elements of the scleraxis gene. Dev Dyn. 2007; 236:1677–1682. [PubMed: 17497702]
17. Murchison ND, Price BA, Conner DA, et al. Regulation of tendon differentiation by scleraxis distinguishes force-transmitting tendons from muscle-anchoring tendons. Development. 2007; 134:2697–2708. [PubMed: 17567668]
18. Schweitzer R, Chyung JH, Murtaugh LC, et al. Analysis of the tendon cell fate using scleraxis, a specific marker for tendons and ligaments. Development. 2001; 128:3855–3866. [PubMed: 11585810]
19. Loiselle AE, Bragdon GA, Jacobson JA, et al. Remodeling of murine intrasynovial tendon adhesions following injury: MMP and neotendon gene expression. J Orthop Res. 2009; 27:833–840. [PubMed: 19051246]
20. Lin TW, Cardenas L, Glaser DL, et al. Tendon healing in interleukin-4 and interleukin- 6 knockout mice. J Biomech. 2006; 39:61–69. [PubMed: 16271588]
21. Richards PJ, Dheer AK, McCall IM. Achilles tendon size and power doppler ultrasound changes compared to MRI: A preliminary observational study. Clin Radiol. 2001; 56:843–850. [PubMed: 11895302]
22. Maffulli N, Longo UG, Franceschi F, et al. Movin and Bonar scores assess the same characteristics of tendon histology. Clin Orthop Relat Res. 2008; 466:1605–1611. [PubMed: 18437501]
23. Cook JL, Feller JA, Bonar SF, et al. Abnormal tenocyte morphology is more prevalent than collagen disruption in asymptomatic athletes' patellar tendons. J Orthop Res. 2004; 22:334–338. [PubMed: 15013093]
24. Abraham T, Carthy J, McManus B. Collagen matrix remodeling in 3-dimensional cellular space resolved using second harmonic generation and multiphoton excitation fluorescence. J Struct Biol. 2009; 171:189–196.
25. Moreaux L, Sandre O, Charpak S, et al. Coherent scattering in multi-harmonic light microscopy. Biophys J. 2001; 80:1568–1574. [PubMed: 11222317]
26. Strupler M, Pena AM, Hernest M, et al. Second harmonic imaging and scoring of collagen in fibrotic tissues. Opt Express. 2007; 15:4054–4065. [PubMed: 19532649]
27. Welch ID, Cowan MF, Beier F, et al. The retinoic acid binding protein crabp2 is increased in murine models of degenerative joint disease. Arthritis Res Ther. 2009; 11:R14. [PubMed: 19173746]
28. Murphy DJ, Nixon AJ. Biochemical and site-specific effects of insulin-like growth factor I on intrinsic tenocyte activity in equine flexor tendons. Am J Vet Res. 1997; 58:103–109. [PubMed: 8989505]
29. Sarkar K, Uhthoff HK. Ultrastructure of the common extensor tendon in tennis elbow. Virchows Arch A Pathol Anat Histol. 1980; 386:317–330. [PubMed: 7445420]
30. Scott A, Cook JL, Hart DA, et al. Tenocyte responses to mechanical loading in vivo: A role for local insulin-like growth factor 1 signaling in early tendinosis in rats. Arthritis Rheum. 2007; 56:871–881. [PubMed: 17328060]
31. Salingcarnboriboon R, Yoshitake H, Tsuji K, et al. Establishment of tendon-derived cell lines exhibiting pluripotent mesenchymal stem cell-like property. Exp Cell Res. 2003; 287:289–300. [PubMed: 12837285]

32. Liden M, Movin T, Ejerhed L, et al. A histological and ultrastructural evaluation of the patellar tendon 10 years after reharvesting its central third. Am J Sports Med. 2008; 36:781–788. [PubMed: 18192494]

33. Zipfel WR, Williams RM, Christie R, et al. Live tissue intrinsic emission microscopy using multiphoton-excited native fluorescence and second harmonic generation. Proc Natl Acad Sci USA. 2003; 100:7075–7080. [PubMed: 12756303]

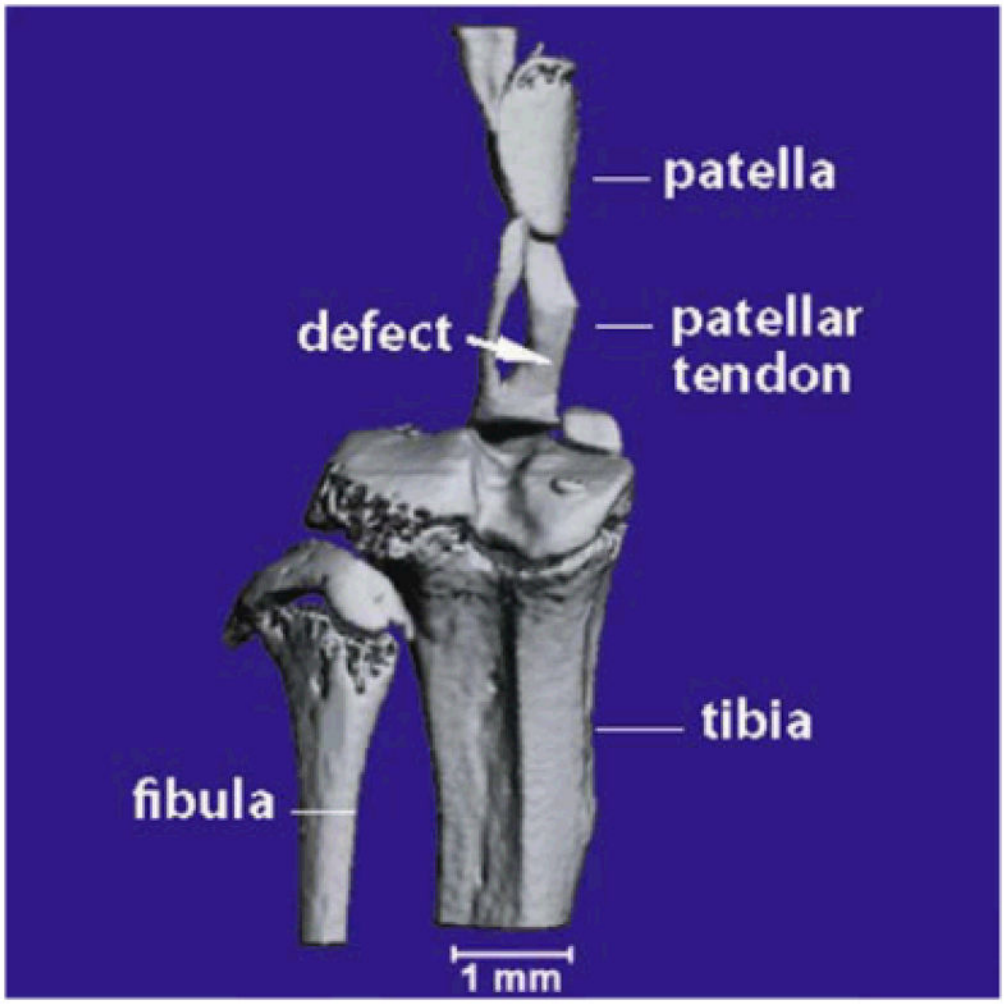

Figure 1.
MicroCT of right mouse patellar tendon. A representative scan illustrating the nature and location of the central defect immediately following injury.

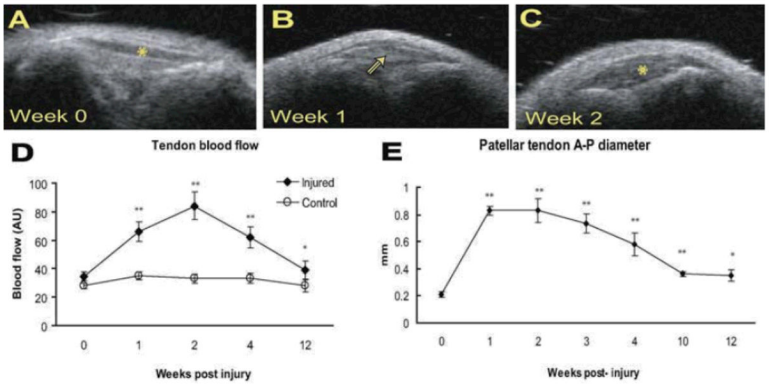

Figure 2.

Noninvasive measurement of patellar tendon pathology. Top panels (A–C) demonstrate evolving ultrasound appearance of a mouse patellar tendon before (week 0) and after (weeks 1, 2) injury. (A) Tendon denoted by asterisk. (B) Hypoechoic area corresponding to sight of defect marked with arrowhead. (C) Tendon marked by asterisk—note substantial tendon thickening. (D,E) Tendon thickness and blood flow gradually decreased over time but remained significantly increased at 12 weeks ($p<0.001$ for thickness, $p=0.0312$ for blood flow).

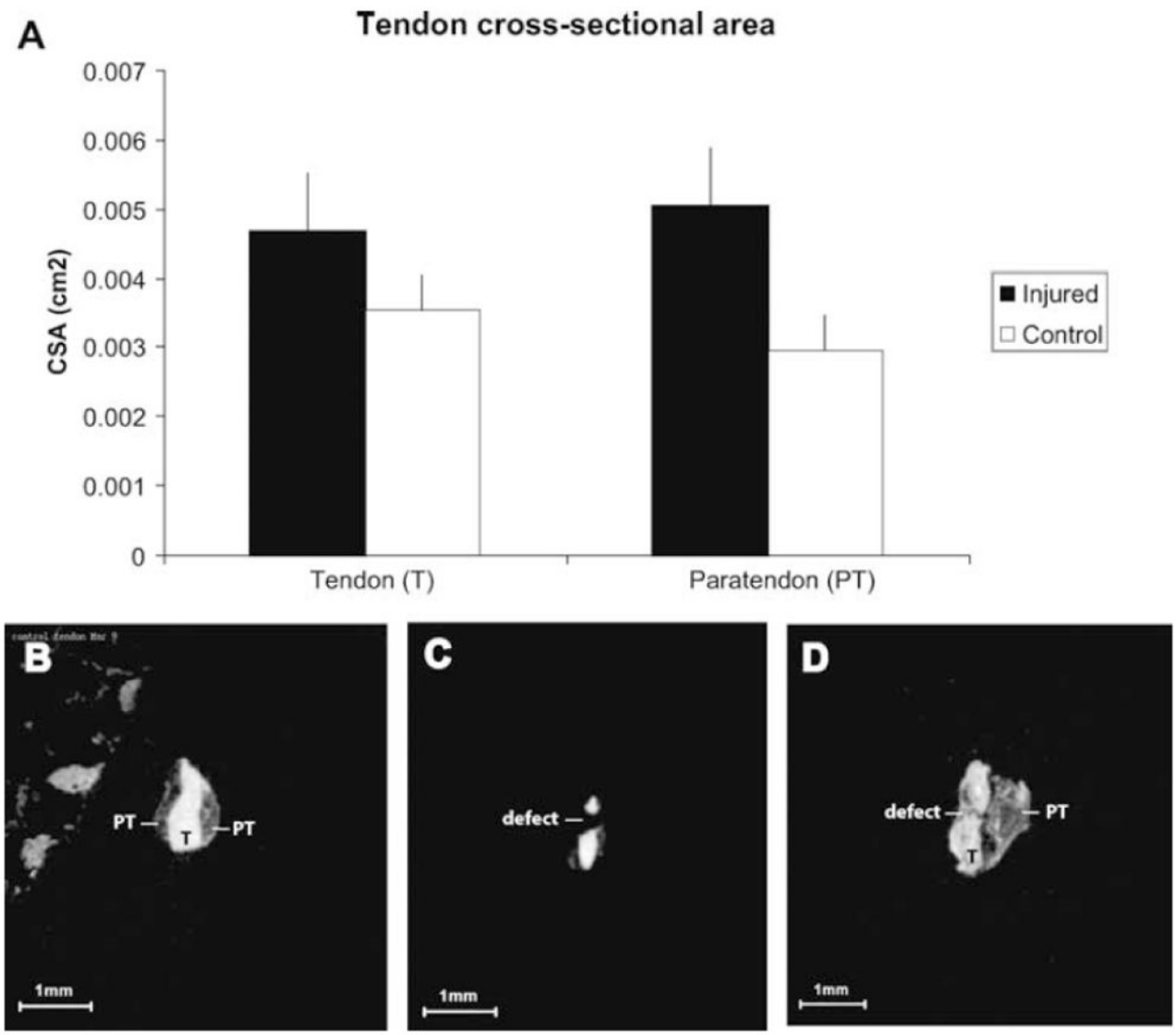

Figure 3.

MicroCT analysis of tendon and paratendon. (A) At 4 weeks, both tendon and paratendon were significantly greater in crosssectional area (CSA). *$p<0.05$. Lower panels: Representative microCT images of tendon that is uninjured (B), immediately post-injury (C), and 3 days following injury (D). In D, substantial thickening can be appreciated both in the tendon (T) and paratendon (PT). Note the in homogenous texture of tendon and paratendon, as well as the irregularity of tendon and paratendon boundaries.

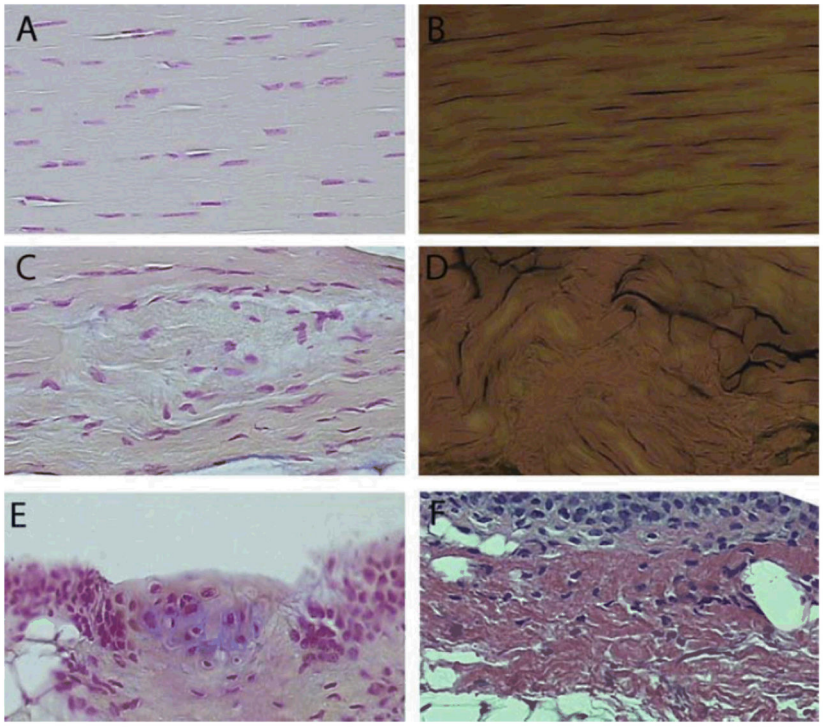

Figure 4.

Histology of injured and uninjured tendon. Uninjured tendon demonstrated regular cellularity (A, fast nuclear red [FNR]) and ordered collagen (B, picrosirius red [PSR]). Sixteen weeks following injury, areas of cellular (C, FNR) and collagen (D, PSR) disarray were prevalent. Other abnormalities present in injured, but not in control, tendon included fibrocartilage metaplasia (E, FNR and Alcian Blue) and expansion of paratendon (F, H&E). In E, note the area of glycosaminoglycan accumulation (blue staining) surrounding chondrocyte-like cells. All images at same scale, original magnification, ×400.

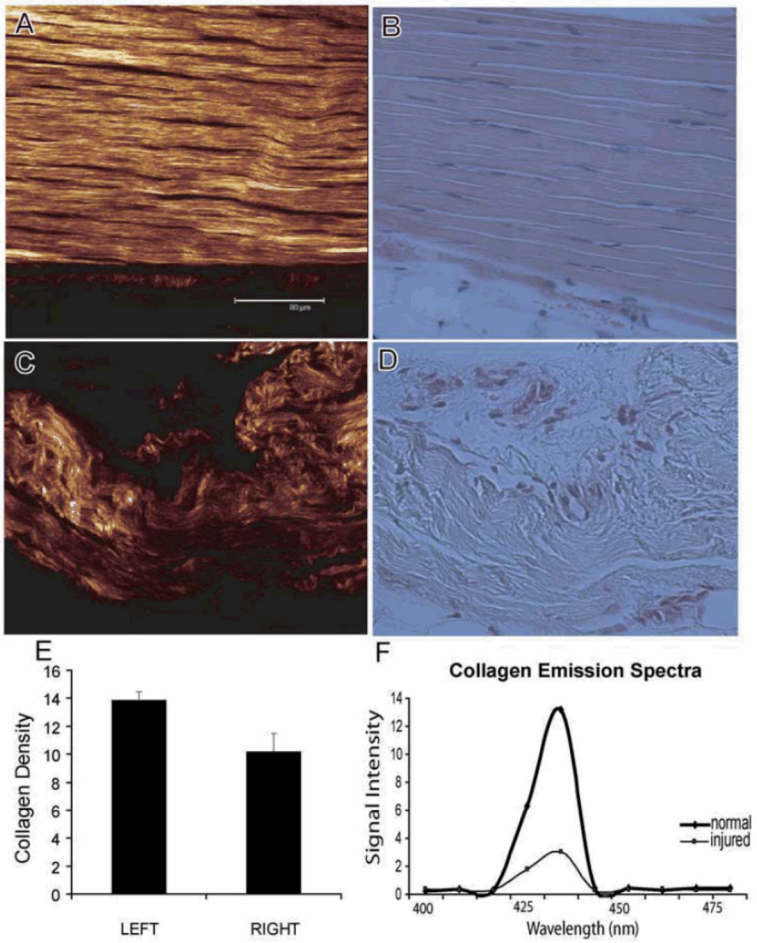

Figure 5.

Representative second harmonic generation (SHG: A,C) and corresponding histological images (H&E: B,D) of normal and injured tendon tissues. The scale bar in A is 80.0 _m, and all images are at the same scale. (E)We observe that the collagen density in the active repair area is significantly reduced compared to uninjured tendons (p=0.004). (F) A representative histogram of the detected SHG signal demonstrates the distribution of the collagen molecular density obtained from normal tendon as well as the one undergoing active repair. The detected SHG signal is clearly manifested by a narrow peak and is spectrally clean, arising only at the expected wavelength of 440 nm. Considerable differences in the collagen matrix are observed between the normal and injured tendon tissues.

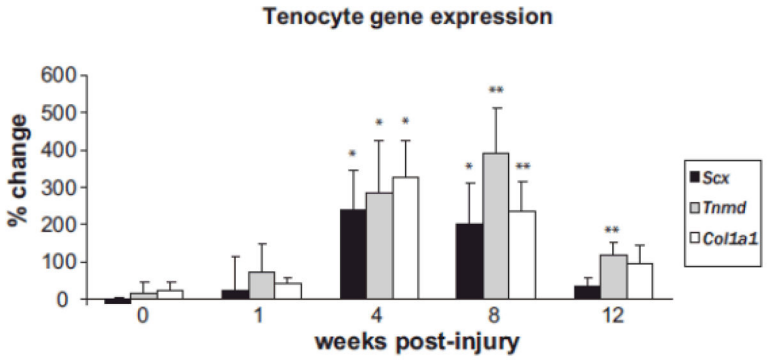

Figure 6.

Gene expression in injured patellar tendon. Values are normalized to 18S rRNA, and compared to control patellar tendon from the same animal and expressed as % change. Scx, Scleraxis; Tnmd, tenomodulin; Col1a1, collagen type 1a1. *p<0.0.05, **p<0.01. n=8 tendons per data point.

Table 1

Primer sequences for qPCR

Gene	Forward Primer	Reverse Primer
Scx	TTGAGCAAAGACCGTGACAGA	TGT GGA CCC TCC TCC TTC TAA C
Col1a1	CTTCACCTACAGCACCCTTGTG	TTGGTGGTTTTGTATTCGATGACT